J Solid State Electrochem (2012) 16:1849–1856
DOI 10.1007/s10008-011-1567-5

ORIGINAL PAPER

In situ neutron powder diffraction studies of lithium-ion batteries

Neeraj Sharma · Vanessa K. Peterson

Received: 31 August 2011 / Revised: 27 September 2011 / Accepted: 3 October 2011 / Published online: 26 October 2011

Abstract Neutron powder diffraction (NPD) offers many advantages in the analysis of battery materials. Understanding the relationship between the structural transformations of electrode materials and their electrochemical performance within lithium-ion batteries is crucial for further development of these technologies and is the overall goal of in situ NPD experiments. In this work, we present NPD data of electrode materials within batteries that are collected in situ during electrochemical cycling, including the commercially available materials $LiCoO_2$, $LiMn_2O_4$, $LiFePO_4$ and graphite and the $YFe(CN)_6$ and $FeFe(CN)_6$ materials that are not commercially available. Using these data, we illustrate the experimental approach and requirements for the collection of in situ NPD data of sufficient quality for detailed structural analyses of the electrode components of interest within batteries.

Keywords Neutron powder diffraction · Electrode · Rietveld · In situ

Introduction

Lithium-ion batteries power many portable devices and in the future are likely to play a significant role in sustainable-energy systems for transportation. Neutron powder diffraction (NPD) can provide both new insights into the atomic-scale functionality of lithium-ion batteries and complementary information to other experimental methods. Neutron radiation interacts with the atomic nuclei of materials, whereas X-ray radiation and electrons interact with the electrons surrounding the atoms, and consequently NPD provides complementary information to X-ray powder diffraction (XRPD). In the study of lithium-ion battery components, the use of NPD affords isotopic contrast, which has two main advantages for these materials. The first advantage of NPD over XRPD for studying lithium-ion batteries is a higher sensitivity to the atomic parameters of lithium (especially in the presence of compounds containing heavier elements), and the second is a larger contrast between neighbouring elements in the periodic table, e.g. Mn and Fe, which feature coherent neutron-scattering cross-sections of 1.75×10^{24} and 11.22×10^{24} cm^2, respectively [1]. Moreover, using components that are isotopically enriched with ^7Li [2] enhances the NPD signal from lithium since the naturally abundant ^6Li features the relatively large neutron absorption cross-section of 60.384×10^{24} cm^2 (at 1.54 Å), relative to ^7Li with 0.039×10^{24} cm^2 [1]. Another major advantage of NPD that is pertinent to the in situ study of battery materials is the penetration depth of the neutron, which allows all components in a lithium-ion battery to be investigated within the whole battery simultaneously.

In a NPD pattern, the signal-to-noise ratio of an electrode in a battery is affected by the amount of electrode material present relative to other battery components, the isotopic composition of the battery and the battery geometry. The isotopic composition of the battery is of particular importance since many battery components are hydrogen rich, notably the polypropylene or polyethylene separators, electrolyte solutions and polymeric coating of the battery housing. Hydrogen is detrimental to the signal-to-noise ratio of the NPD data as a consequence of the large incoherent neutron-scattering cross-section (80.260×10^{24} cm^2 [1]) that results in the isotropic scattering of neutrons by the hydrogen nuclei and contributes signifi-

N. Sharma · V. K. Peterson (✉)
Australian Nuclear Science and Technology Organisation,
The Bragg Institute,
Locked Bag 2001,
Kirrawee DC, NSW 2232, Australia
e-mail: vanessa.peterson@ansto.gov.au

cantly to the background in a NPD pattern. The amount of the component of interest that is present in the battery is also an important factor in obtaining a good signal-to-noise ratio of the NPD data. Coin cell-type lithium-ion batteries do not contain enough electrode material to be studied easily in situ using NPD. Larger batteries, such as prismatic, pouch [3] or cylindrical 18650-type [4] batteries, overcome the quantity limitations but introduce a larger quantity of components other than the one of interest to the cell, which can be detrimental to the NPD data.

In situ experimentation is crucial to observing the structural changes [5] in electrode materials within the battery as a function of their electrochemical activity. Time-dependent in situ experiments allow non-equilibrium states of electrode materials and lithium-ion batteries to be measured as the structural detail is continuously probed with or without an applied current [6]. Real-time powder diffraction data provide information concerning the kinetics of structural transitions occurring in non-equilibrium systems, which are closer to real-life conditions. The rate of change of parameters such as lattice parameters in single-phase phase transitions and phase fractions in two-phase phase transitions can all be determined using real-time powder diffraction data, as well as the difference between the rates of change of such parameters in non-equilibrium and equilibrium conditions. In situ studies with insufficient temporal resolution and ex situ studies probe only the equilibrium states of electrode materials as the time required to collect data, and in the case of ex situ data to extract, dry and mount the electrode, may allow the electrode to reach the equilibrium state.

All reported in situ NPD data for battery components use lithium metal as the counter electrode [6–13], where the new material is measured electrochemically against lithium. The first in situ NPD study of a battery material used a cylindrical cell containing a lithium rod enveloped by the separator and approximately 5 g of electrode material encompassed in a Pyrex tube [12, 13]. The cell was successfully used to collect seven NPD patterns during the slow charge of $LiMn_2O_4$ [13]. Peak broadening over the course of the collection time (unreported) and low useable current rates were limitations of this study to the understanding of the electrode structure–function relationship. Another cell used to collect NPD data of battery electrode components within a battery is an enlarged coin cell, where approximately 2.2 g of electrode material and other components are encased in a polymer and used to collect NPD for $LiNiO_2$-type cathodes and $Li_4Ti_5O_{12}$ anodes [8, 11]. Six-hour collection times were required for the cathode materials, with charging times between 20 and 50 h [8]. This cell enabled the evolution of lattice parameters, oxygen positions and ratio of lithiated phases to be followed as a function of charge/discharge [11]. The approach taken in this work was to charge and equilibrate the cell before an open-circuit voltage step was applied during which time NPD data were collected [8, 11]. These data represent snapshots of the battery at different states of charge, even though the voltage is changing during data acquisition. In some work [11], multiple batteries were used to minimize lost neutron instrument time, and data represent not only different states of charge of a battery but different batteries.

All the above studies using in situ powder diffraction for the investigation of lithium-ion batteries are in situ with respect to the component of interest within a battery but not with respect to the electrochemical state of the battery, which has an assumed state-of-charge. The collection times in much of this previous work are relatively large or unreported, with NPD data collected over a period of time during which the battery may be equilibrating in charge or undergoing cycling.

We have developed a roll-over battery design (Fig. 1) that mimics the conventional cylindrical 18650-type [4] batteries but maximizes the signal-to-noise ratio of the component of interest in the NPD data [6, 7, 10]. Using this cell, we have investigated the crystallographic evolution of novel $Li(Co_{0.16}Mn_{1.84})O_4$ cathodes [6] as well as composite $Li_4Ti_5O_{12}/TiO_2$ [10] and MoS_2 anodes [7]. Real-time data were crucial to understanding MoS_2 functionality, where the ex situ NPD patterns of MoS_2 extracted from batteries at a particular state-of-charge are fairly featureless [7]. These featureless patterns can arise as a result of the

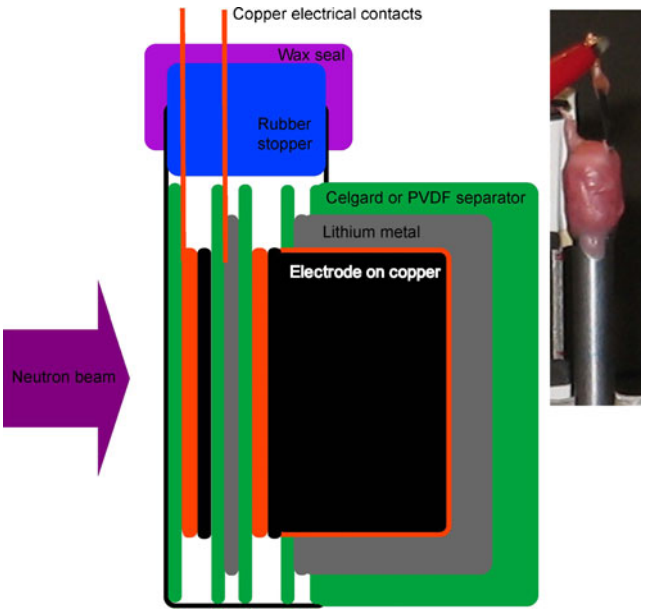

Fig. 1 Cross-section schematic of the roll-over custom-made cell. Layers of separator (*green*), lithium electrode (*grey*) and electrode of interest on copper (*black* and *orange*) are shown. The neutron beam is indicated by the *arrow* on the *left* and a photograph of the cell is shown on the *right-hand side*

degradation of long-range order (crystalline structure) as a direct consequence of the extraction method. Using our cell, evolution of the structure of the MoS_2 was tracked using in situ NPD during the course of discharge, allowing this loss of long-range order to be unambiguously assigned to lithium insertion processes that do not adversely affect battery performance [7]. Time-dependent in situ NPD data allowed the characterisation and comparison of the current-free and current-applied discharge processes in the $LiCo_{0.16}Mn_{1.84}O_4$ cathode [6]. In situ NPD data of the composite $Li_4Ti_5O_{12}/TiO_2$ electrode illustrated that both components in the composite are electrochemically active but that each component is active at a certain voltage, allowing the selective Li insertion/extraction of each component [10].

In the following sections, we show how the NPD can be used to study lithium-ion batteries in situ and in real time using examples of previously unreported in situ NPD work using the high-intensity neutron powder diffractometer, WOMBAT [14]. Using these examples, we detail the requirements for the collection of NPD data of electrode materials during their electrochemical cycling in batteries with a good signal-to-noise ratio.

Experimental

NPD data were collected for electrode materials in commercially available cells without modification or in our roll-over cell design. Electrodes used in the roll-over cell design are made by mixing the material of interest with *n*-methyl 2-pyrrolidone, carbon black and polyvinylidene fluoride (PVDF) to form a paste that is applied to an aluminium sheet, made to a thickness of 400 μm and which is then dried in a vacuum oven. *n*-Methyl 2-pyrrolidone is removed during the drying process. The cell is assembled in an argon glove box with layers of materials arranged in the following order: PVDF, electrode paste on aluminium, PVDF and lithium metal. Copper wires are placed in contact with both electrodes. The assembly is rolled using the outer PVDF layer and inserted into a 6- or 9-mm diameter vanadium can. The electrolyte is composed of 1 M lithium hexafluorophosphate ($LiPF_6$) dissolved in a 1:1 vol. % mixture of deuterated ethylene carbonate and deuterated dimethyl carbonate, with conventional hydrogenated electrolytes sometimes used. The electrolyte is added dropwise to the vanadium can which is subsequently sealed with wax.

In situ NPD data were collected on WOMBAT, the high-intensity powder diffractometer, at the Open Pool Australian Light-water (OPAL) reactor facility at the Australian Nuclear Science and Technology Organisation (ANSTO) [14]. NPD data were collected for periods of 2 to 20 min over the course of two or more days, depending on the sample and the applied charging/discharging rates. Data were collected in the scattering angle range $16 \leq 2\theta \leq 136°$ and with a wavelength (λ) of 2.41 Å which was determined accurately for each experiment using the Al_2O_3 NIST SRM 676. WOMBAT features an area detector covering 120° in scattering angle (2θ), effectively enabling diffraction data to be continuously collected from batteries during electrochemical cycling in galvanostatic mode with applied currents ranging from ±1 mA to 2 A using an Autolab potentiostat/galvanostat (PG302N).

Data correction and reduction were undertaken using the programme LAMP [15]. Rietveld refinements were carried out using the GSAS [16] suite of programmes with the EXPGUI [17] interface.

Results and discussion

In order to understand the link between the battery electrochemistry and the corresponding structural evolution of the battery components, the time-dependent electrochemical activity of the battery must be considered. There are two approaches for collecting in situ NPD data of lithium-ion batteries: The first is to use commercially available batteries, and the second is to use custom-made batteries that mimic their commercial counterparts but are better adapted to the neutron experiment.

NPD studies of commercial lithium-ion batteries

The relationship between crystal structure and electrochemical properties of battery components, derived from in situ experiments on commercial lithium-ion batteries, can be related directly to the performance of the battery studied. A temporal collation of 730 NPD patterns, each collected over a period of 2 min, for a commercial lithium-ion battery composed of a graphitic anode and $LiCoO_2$ cathode is shown in Fig. 2. Changes in the scattering angle (2θ) of the $LiCoO_2$ and graphite peaks are observed as a function of time. In particular, the graphite anode shows a second phase forming near the charged state of the battery with a reflection appearing and disappearing just below $2\theta = 38°$. The influence of applied current rate can also be discerned with higher current rates leading to faster structural changes. The first NPD pattern is presented in Fig. 3a and the Rietveld refinement of structural models with this pattern is presented in Fig. 3b, and via sequential refinements we can extract the evolution of structural parameters. Figure 2b shows the evolution of the graphitic *c* lattice parameter corresponding to the NPD data in Fig. 2a and the variation in the measured battery voltage. Correlations between voltage or electrochemical properties and crystallographic parameters can be obtained with these data [5, 18].

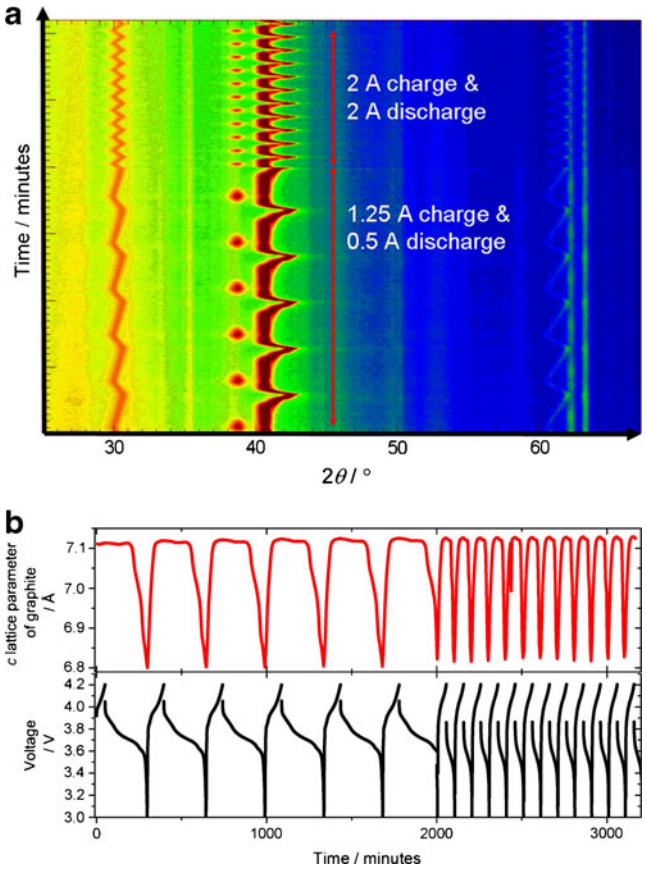

Fig. 2 **a** A series of NPD patterns from a commercial $LiCoO_2$ || graphite cylindrical battery collected in 2-min intervals plotted as a function of time. The *colour* represents intensity and two different charge and discharge rates are employed. The feature at ~30° is related to the $LiCoO_2$ cathode, while the feature at ~40° is related to graphite. Further reflections can be determined from Fig. 3b which is a Rietveld refined fit to the first NPD pattern in this series. **b** The evolution of the *c* lattice parameter of graphite (*red*) determined from sequential Rietveld refinements of structural models with the NPD data in **a** and the measured voltage (*black*)

Commercial batteries are optimized for electrochemical performance and not for neutron diffraction experiments. In the best-case scenario, a good NPD signal can be obtained for a material of interest from within a commercially available battery. The NPD signal from the crystalline components within a battery is dependent on the battery geometry and composition; the latter includes the isotopic composition and structure of all components in the battery. All these factors are pre-determined in commercial batteries and affect the signal-to-noise ratio of the NPD data. The amount of the component of interest that is present in the battery is also an important factor in obtaining a good signal-to-noise ratio of the NPD data.

Commercially manufactured cathode materials are, at present, limited to $LiCoO_2$, $LiFePO_4$ and $LiMn_2O_4$, while anode materials are either graphite or lithium. NPD patterns collected using WOMBAT of $LiCoO_2$ (2 min), $LiFePO_4$ (5 min) and $LiMn_2O_4$ (5 min) in commercial batteries containing graphite anodes are shown in Fig. 3. The Rietveld-model fits to these data are also shown in Fig. 3.

Neutrons are attenuated by the battery as a result of the presence of hydrogen and neutron-absorbing isotopes such as the naturally occurring isotopes of lithium, cobalt and manganese. Figure 3 reveals the effect that the cell geometry, in conjunction with the neutron attenuation, has on the background in the NPD patterns as a consequence of the different path lengths for the neutrons into and out of the sample, which result in a scattering angle-dependent background. This problem is compounded by the inhomogeneous battery construction, which can result in the best signal from the component of interest being obtained when the sample is not centred with respect to the scattering centre of the detector. The NPD pattern from the annular battery in Fig. 3a features a prominent dip in the background at approximately the centre of the detector (at a scattering angle of 90°) as a result of the sample alignment. The NPD data of the prismatic batteries (Fig. 3c, e) feature a sloping background as a result of their geometry. The slight rise in the background at lower scattering angles, between approximately 20° and 45° in Fig. 3a–e, is a broad contribution from the semi-amorphous graphitic anode to the NPD data. These features are treated as a background in the Rietveld model (Fig. 3b, d, f), which enable insight into the crystal structure transitions of the crystalline electrode materials of interest during charge/discharge [9, 18].

Custom-made lithium-ion batteries

Batteries that are custom-made for NPD investigation of electrode materials are used where NPD data sufficient for analysis cannot be obtained from commercially available batteries or where commercially available batteries do not exist for the electrode materials of interest, such as for newly synthesized electrode materials or electrode materials made in relatively small quantities.

Many of the obstacles presented by commercial lithium-ion batteries for the collection of NPD data can be overcome by the use of custom-made lithium-ion batteries. Custom-made lithium-ion batteries are designed to optimize the signal-to-noise ratio of NPD data from battery components of interest whilst maintaining the electrochemical properties and functionality of new materials in a battery.

Our roll-over cell design (Fig. 1) features a vanadium can as the battery housing, which has relatively little coherent neutron scattering, minimizing the contribution to the (flat) background in the NPD data from the housing. To maximize the signal-to-noise ratio of the NPD data for the component of interest, we minimize hydrogen content

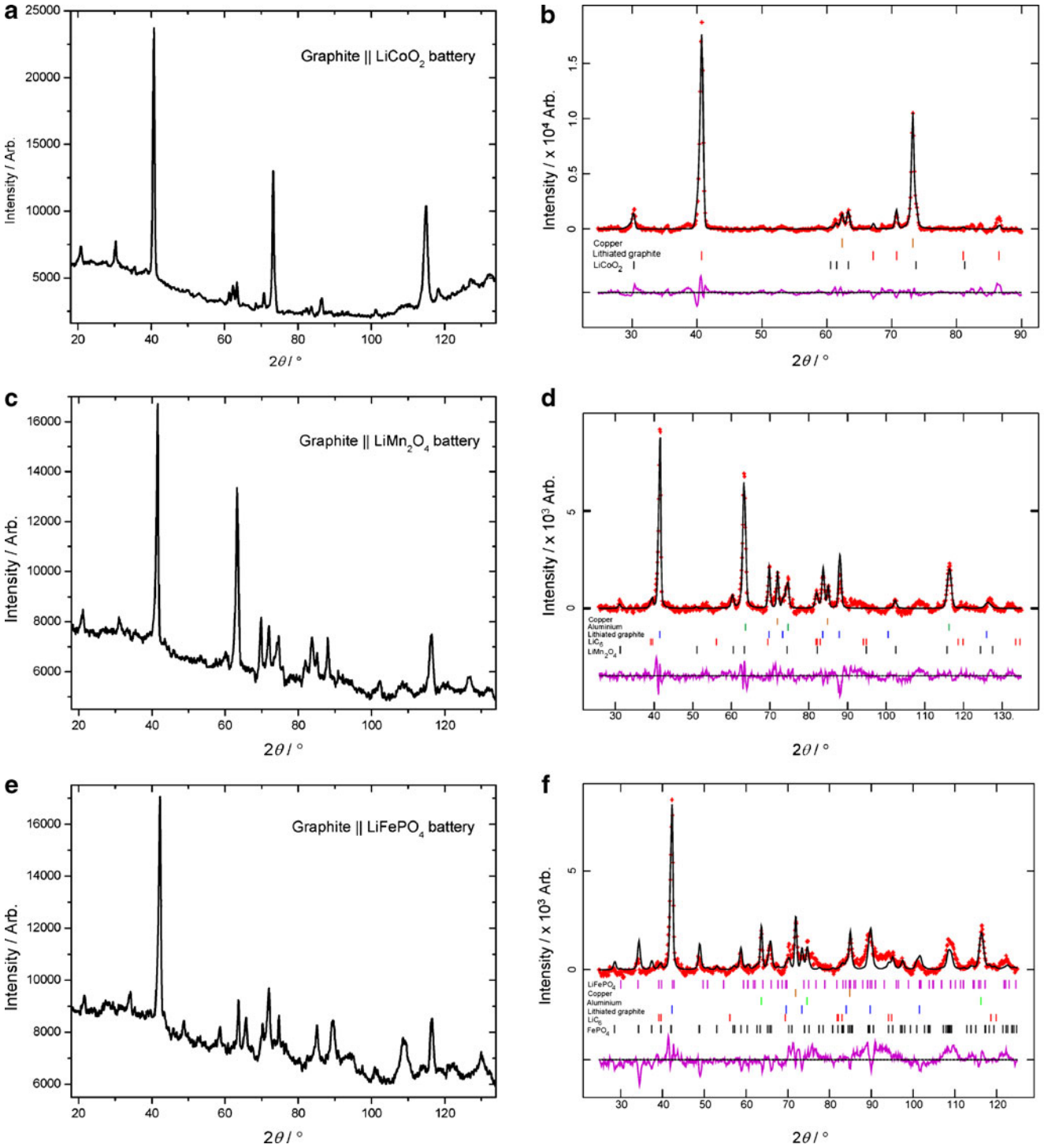

Fig. 3 NPD patterns of commercially available batteries collected on WOMBAT at $\lambda \cong 2.41$ Å, where 2θ is the scattering angle: **a** a 2-min NPD pattern of a cylindrical 18650-type graphite || $LiCoO_2$ battery, **b** Rietveld refinement fit to the NPD pattern in **a**, **c** a 5-min NPD pattern of a prismatic graphite || $LiMn_2O_4$ battery, (d) Rietveld refinement fit to the NPD pattern in **c**, **e** a 5-min NPD pattern of a prismatic graphite || $LiFePO_4$ battery and **f** Rietveld refinement fit to the NPD pattern in **e**. These batteries are purchased at a state-of-charge of around 60%. The data shown in **a**, **c** and **e** are directly comparable as the same data collection and correction procedures were applied to each dataset

by using a particular electrolyte solution that consists of $LiPF_6$ dissolved in deuterated carbonates (ethylene and dimethyl carbonate in various mixtures) and polyvinyl difluoride separators.

We investigated coordination framework materials as cathodes using the roll-over cell design. Figure 4 shows NPD patterns collected for 20 min using WOMBAT for identical cathode materials in a 6-mm-diameter cell

(Fig. 4a; ≅200 mg of cathode material) and in a 9-mm-diameter cell (Fig. 4b; ≅500 mg of cathode material). Figure 4c shows NPD data collected for 10 min using WOMBAT for a cathode material that is similar to that shown in Fig. 4a, b but with a different battery composition in a 9-mm diameter cell. A 20-min NPD pattern using the 6-mm cell does not match the intensity obtained from the 20-min NPD pattern from a 9-mm cell, a direct consequence of the quantity of material in the neutron beam. Despite the significantly higher amount of cathode material in the 9-mm cell relative to the 6-mm cell, the signal-to-noise ratios of the data from the cathode are comparable between both cells as a result of two factors. The first is due to the use of the PVDF separator in the 6-mm cell (Fig. 4a), as opposed to the Celgard separator used in the 9-mm cell (Fig. 4b), with the latter containing significantly more hydrogen. The second factor is the relatively larger quantity of all battery components in the 9-mm cell compared with the 6-mm cell, including separator and electrolyte solution, which can adversely affect the signal-to-noise ratio of the component of interest. A comparison of 9-mm cells with Celgard separators containing conventional hydrogenated electrolyte solution (Fig. 4b) and those containing deuterated electrolyte solution (Fig. 4c) allows the influence of deuteration on the NPD signal to be shown. Although the diffraction patterns in Fig. 4b, c look similar, the signal-to-noise ratio of the data for the cathode is approximately double in the cell containing deuterated electrolyte. This is particularly relevant as the NPD data for the cell containing deuterated electrolyte were collected in half the time of the cell containing hydrogenated electrolyte.

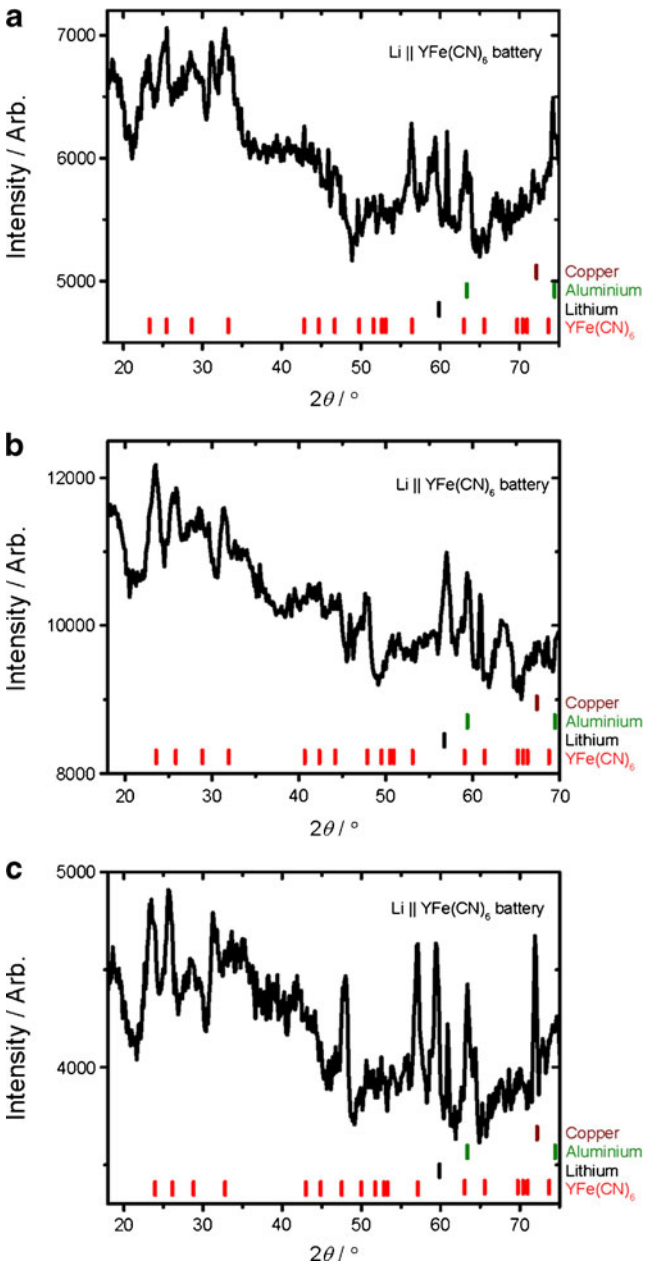

Fig. 4 Selected regions of NPD data collected on WOMBAT using $\lambda \cong 2.41$ Å, where 2θ is the scattering angle, using a customized roll-over-type Li || $YFe(CN)_6$ battery. **a** A 20-min NPD pattern of a 6-mm diameter cell containing PVDF separator, commercial (hydrogenated) electrolyte and≅200 mg of $YFe(CN)_6$. **b** A 20-min NPD pattern of a 9-mm diameter cell containing Celgard separator, hydrogenated electrolyte and≅500 mg of $YFe(CN)_6$. **c** A 10-min NPD pattern of a 9-mm diameter cell containing Celgard separator, deuterated electrolyte and≅500 mg of $YFe(CN)_6$

An indication of data quality is shown by the flatness of the background, which is improved in Fig. 4c relative to Fig. 4a, b, all of which show a non-uniform background contribution. Therefore, we find that both deuteration of the electrolyte solution and use of the PVDF membranes have a marked effect on the signal-to-noise ratios of NPD data for the material of interest. Replacing Celgard with glass fibre separators would remove hydrogen altogether from the

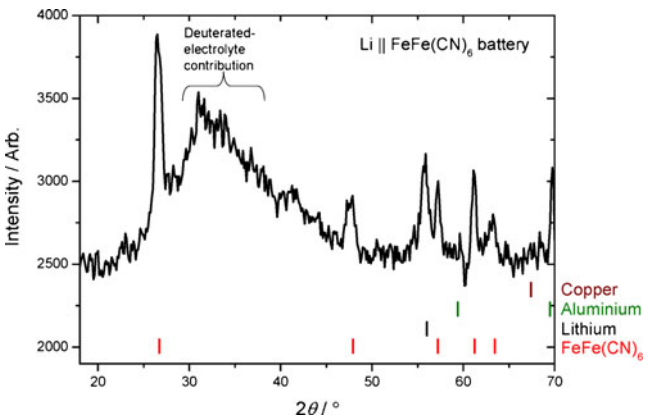

Fig. 5 Selected region of a 5-min NPD pattern collected on WOMBAT using $\lambda \cong 2.41$ Å for a customized roll-over-type Li || $FeFe(CN)_6$ battery. This 9-mm diameter cell contains ≅300 mg of $FeFe(CN)_6$, deuterated electrolyte and PVDF separator

separator. Unfortunately, glass fibre is brittle, leading to a higher probability of cathode and anode contact (i.e. short circuits) in the roll-over battery design. Although the electrolyte solution wets the PVDF membrane better than the Celgard, the PVDF membrane is thicker than the Celgard, which in turn reduces the overall amount of cathode material that can be packed into cells of a fixed diameter. Therefore, using PVDF reduces not only the amount of hydrogen in the neutron beam but also the amount of cathode material in the beam, although the overall gain in signal-to-noise ratio of the NPD data for the cathode justifies the use of PVDF.

It is important to test the electrochemical performance of the modified cells used for in situ NPD experiments using offline tests in order to assess the impact of the cell modification on electrode performance. The combination of Celgard separator and conventional hydrogenated electrolyte solution has been optimized over the course of lithium-ion battery research and almost all commercial batteries use this combination. To quantify the effects of electrolyte deuteration, which may affect charge transfer processes through the electrolyte as a consequence of a mass isotope effect, offline coin cell testing is performed [6]. We find a small but significant difference in the cell performance between cells that use deuterated electrolytes and those using conventional, hydrogenated electrolytes. Deuteration of the electrolyte improves the signal-to-noise ratio of NPD data from the electrode in the battery. The hydrogen isotope deuterium has a significantly larger coherent neutron scattering length than hydrogen, enhancing the contribution of the liquid structure factor for the electrolyte to the NPD signal. The electrolyte is most noticeable in Fig. 5, which shows a NPD pattern collected in 5 min for approximately 300 mg $FeFe(CN)_6$ cathode material within a 9-mm-diameter cell containing both deuterated electrolytes and PVDF separator.

Cells for use in the collection of in situ NPD data are being improved and new types of cells are being tested for this purpose, including modified Swage-lok-type cells and all-solid-state lithium-ion batteries. Our focus for future cells designed for the collection of in situ NPD data is the use of hydrogen-free solid-state electrolytes, which mitigate problems associated with deuteration and remove entirely the requirement for separators.

Summary

The difficulties in collecting in situ NPD data from lithium-ion batteries arise from the presence of hydrogen-rich electrolyte and separator, neutron absorption by naturally abundant isotopes including ^{6}Li, the often small amount of electrode of interest that is present and the battery geometry. We have shown that custom-made batteries with similar performance to their commercial or conventional coin cell counterparts can be constructed relatively inexpensively and used to collect high-quality NPD data from lithium-ion batteries. Critical aspects of this custom-made cell design include a cylindrical geometry and the minimization of hydrogen within the battery. Such a design allows novel electrode materials to be tested in situ and in real time to correlate the structural evolution of electrodes with the electrochemical performance of the battery, including in non-equilibrium states of the battery. The design and construction of this battery allow the electrochemical behaviour of electrodes with novel chemistries and often unknown delithiation/lithiation mechanisms to be explored. Using high-intensity neutron powder diffractometers, such as WOMBAT at OPAL, in conjunction with a cell design that maximizes the neutron scattering signal, we can examine relatively small quantities of weakly scattering electrode materials to understand the mechanism of electrode and battery function.

Acknowledgments The infrastructure and materials for the experiments were in part provided by the ANSTO-funded 'Energy project' within the Bragg Institute. We thank Mark Beamish from Siomar Battery Engineering for providing the $LiCoO_2$ battery and Yuping Wu (Fudan University, China) for providing the $LiFePO_4$ and $LiMn_2O_4$ batteries. We also acknowledge Rosalind Gummow (James Cook University), Guodong Du (University of Wollongong), Zaiping Guo (University of Wollongong), Sam Duyker (University of Sydney), Lisa Cameron (University of Sydney) and Cameron Kepert (University of Sydney) for their work on the examples presented.

References

1. Sears VF (1992) Neutron News 3:29–37
2. Nishimura S, Kobayashi G, Ohoyama K, Kanno R, Yashima M, Yamada A (2008) Nature Mater 7:707–711
3. Lampe-Onnerud C, Thomas JO, Hardgrave M, Yde-Andersen S (1995) J Electrochem Soc 142:3648–3651
4. Commission IE (2001) Secondary lithium cells and batteries for portable applications. IEC 61960–2:2001
5. Isnard O (2006) J Optoelectron Adv Mater 8:411–417
6. Sharma N, Reddy MV, Du G, Adams S, Chowdari BVR, Guo Z, Peterson VK (2011) J Phys Chem C. http://dx.doi.org/10.1021/jp2026237
7. Sharma N, Du G, Studer AJ, Guo Z, Peterson VK (2011) Solid State Ionics 199–200:37–43
8. Rosciano F, Holzapfel M, Scheifele W, Novak P (2008) J Appl Cryst 41:690–694
9. Rodriguez MA, Ingersoll D, Vogel SC, Williams DJ (2004) Electrochem Solid-State Lett 7:A8–A10
10. Du G, Sharma N, Kimpton JA, Jia D, Peterson VK, Guo Z (2011) Adv Funct Mater. doi:10.1002/adfm.201100846
11. Colin J-F, Godbole V, Novak P (2010) Electrochem Comm 12:804–807
12. Bergstom O, Andersson AM, Edstrom K, Gustafsson T (1998) J Appl Cryst 31:823–825

13. Berg H, Rundlov H, Thomas JO (2001) Solid State Ionics 144:65–69
14. Studer AJ, Hagen ME, Noakes TJ (2006) Physica B 385–386:1013–1015
15. Richard D, Ferrand M, Kearley GJ (1996) J Neutron Research 4:33–39
16. Larson AC, Von Dreele RB (1994) General Structure Analysis System (GSAS). Los Alamos National Laboratory Report LAUR 86–748
17. Toby BH (2001) J Appl Cryst 34:210–213
18. Sharma N, Peterson VK, Elcombe MM, Avdeev M, Studer AJ, Blagojevic N, Yusoff R, Kamarulzaman N (2010) J Power Sources 195:8258–8266